

# Screen-Printed Washable Electronic Textiles as Self-Powered Touch/Gesture Tribo-Sensors for Intelligent Human–Machine Interaction

Ran Cao,<sup>†,‡</sup> Xianjie Pu,<sup>§</sup> Xinyu Du,<sup>†,‡,¶</sup> Wei Yang,<sup>†,‡</sup> Jiaona Wang,<sup>\*,†,||</sup> Hengyu Guo,<sup>\*,†,‡</sup> Shuyu Zhao,<sup>†,||</sup> Zuqing Yuan,<sup>†,‡,¶</sup> Chi Zhang,<sup>†,‡,¶</sup> Congju Li,<sup>\*,†,‡,¶</sup> and Zhong Lin Wang<sup>†,‡,||,¶</sup>

<sup>†</sup>Beijing Institute of Nanoenergy and Nanosystems, Chinese Academy of Sciences, Beijing 100083, China

<sup>‡</sup>School of Nanoscience and Technology, University of Chinese Academy of Sciences, Beijing 100049, China

<sup>§</sup>Department of Applied Physics, Chongqing University, Chongqing 400044, China

<sup>⊥</sup>School of Materials Science & Engineering, Beijing Institute of Fashion Technology, Beijing 100029, China

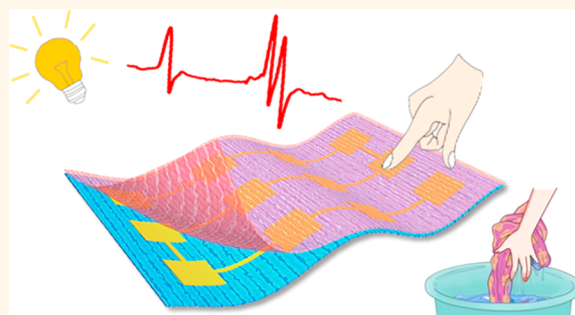
<sup>||</sup>Beijing Key Laboratory of Clothing Materials R&D and Assessment, Beijing 100029, China

<sup>¶</sup>School of Materials Science and Engineering, Georgia Institute of Technology, Atlanta, Georgia 30332-0245, United States

## Supporting Information

**ABSTRACT:** Multifunctional electronic textiles (E-textiles) with embedded electric circuits hold great application prospects for future wearable electronics. However, most E-textiles still have critical challenges, including air permeability, satisfactory washability, and mass fabrication. In this work, we fabricate a washable E-textile that addresses all of the concerns and shows its application as a self-powered triboelectric gesture textile for intelligent human–machine interfacing. Utilizing conductive carbon nanotubes (CNTs) and screen-printing technology, this kind of E-textile embraces high conductivity (0.2 kΩ/sq), high air permeability (88.2 mm/s), and can be manufactured on common fabric at large scales. Due to the advantage of the interaction between the CNTs and the fabrics, the electrode shows excellent stability under harsh mechanical deformation and even after being washed. Moreover, based on a single-electrode mode triboelectric nanogenerator and electrode pattern design, our E-textile exhibits highly sensitive touch/gesture sensing performance and has potential applications for human–machine interfacing.

**KEYWORDS:** *electronic textiles, washable, self-powered, human–machine interaction*



Rapid advancements in wearable electronics have imposed urgent demands for electronic textiles (E-textiles).<sup>1,2</sup> As a critical component of E-textiles, an electrode with a designable pattern still meets great challenges from mechanical and chemical stability aspects.<sup>3,4</sup> Compared with traditional stiff electrodes, a conductive network constructed by nanoparticles, nanofibers, or nanotubes is preferred for fabricating electrodes on textiles.<sup>5,6</sup> Some related works have been reported about the electrode on the basis of textiles with nanomaterials through dip-coating,<sup>7</sup> chemical deposition,<sup>8</sup> and magnetron sputtering.<sup>9</sup> However, these processing methods can hardly meet the requirements of washability, pattern diversity, and time-efficient/mass production of the electrode. On the other hand, smart systems for touch/gesture sensing are crucial for human–machine interfaces.<sup>10,11</sup> The realization of gesture control through E-textiles requires highly integrated sensors, which sets higher

requirements for the formation of electrode patterns. Furthermore, the development of such E-textiles is also shadowed by its power supply as a traditional battery is a burden for light, convenient E-textiles.<sup>12</sup>

Newly invented triboelectric nanogenerators (TENGs), on the basis of triboelectrification effect and electrostatic induction, have superiority in converting low-frequency mechanical energy into electric power.<sup>13,14</sup> With advantages like universal material, simple structure, low cost, easy fabrication, and prominent stability, the TENG has attracted considerable interest in wearable electronics.<sup>15–17</sup> Moreover, fabrics or fibers can be easily weaved into textiles to manufacture TENGs for harvesting human mechanical energy.<sup>18–20</sup> For example, Wen

Received: April 3, 2018

Accepted: May 17, 2018

Published: May 17, 2018

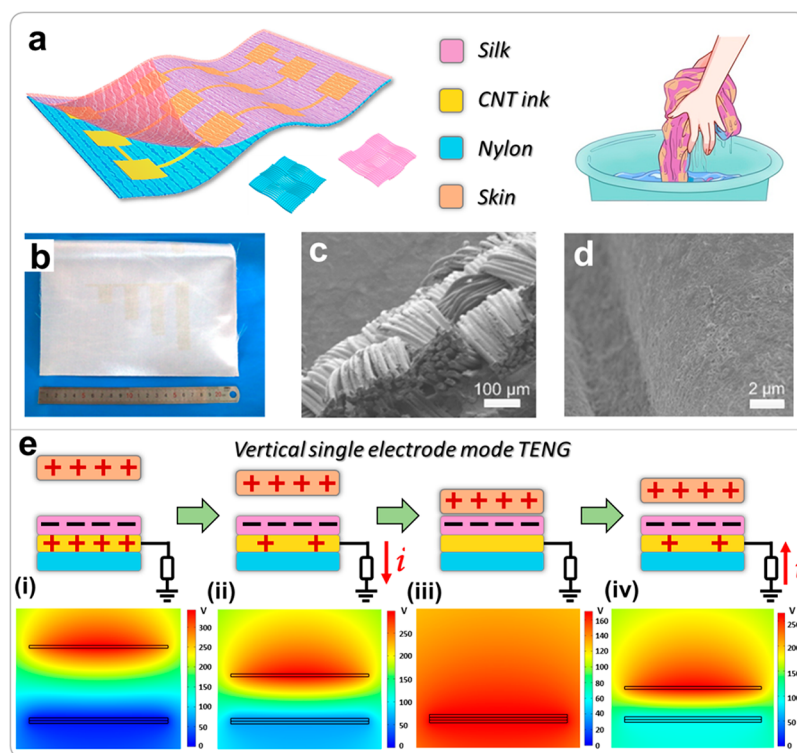


**Figure 1.** Structure design and sensing mechanism of the washable electronic textile (WET). (a) Schematic illustration of WET with an array of CNT electrodes by screen printing. (b) Digital photograph of the large-scale WET. (c,d) SEM images of the surface of the textile with CNT ink on it. (e) Short-circuit charge distribution (top) and open-circuit potential distribution (bottom) show the sensing mechanism of the WET.

*et al.* have reported a hybridized self-charging power textile system by knitting a fiber-shaped TENG with a fiber-shaped storage device (capacitor) into pieces of clothes.<sup>21</sup> Moreover, the TENG can also act as a self-powered sensor for mechanical trigger detection with advantages of promising sensitivity and high signal level.<sup>22,23</sup> Therefore, combining electrode materials, E-textiles based on a TENG is the most promising approach for realizing self-powered wearable multifunctional sensors.

In this work, a washable electronic textile (WET) used as a self-powered touch/gesture sensor was developed through screen-printing for intelligent human–machine interfacing. With the utilization of a flexible textile substrate, the electrode formed by carbon nanotubes (CNTs) exhibits excellent performance under harsh mechanical deformation (*e.g.*, washing). In addition, the effect of CNT ink thickness on both the conductivity of the electrode and the air permeability of the textile was systematically studied. Based on a single-electrode mode TENG, the fabricated WET shows high sensitivity, fast response time, and stable cycle performance to external mechanical force. The application of a designable WET in accessing different software on a computer was demonstrated. Moreover, home appliances such as light bulbs, electric fans, microwave ovens, and so forth can be controlled wirelessly by simply pressing the WET. Features like air permeability, cost efficiency, high sensitivity, good washability, and mass production of the WET promise its wide application in smart textiles and intelligent human–machine interactions.

## RESULTS AND DISCUSSION

As illustrated in Figure 1a, the washable E-textile (WET) is mainly constructed of three layers. The top layer is silk fabric, serving as one frictional material; the bottom layer is nylon

fabric, which is regarded as the substrate, and the middle layer is the CNT electrode array. The electrode array fabricated by the CNT ink was printed on nylon fabric. In order to realize the washability of the electrode, polyurethane (PU) was added in the synthesis procedure of the CNT ink. According to the chemistry structure formulas listed in Figure S1a in the Supporting Information, hydrogen bonds are formed between amino groups consisting of PU and carbonyl groups within most common textiles. Consequently, the firm adherence between the CNTs and the fabric is ensured even in water. Moreover, the water contact angle of the electrode ( $82^\circ$ ) is provided in Figure S1b (Supporting Information). Figure 1b presents the digital photograph of as-fabricated WET in large scale. As shown in Figure 1c, the scanning electron microscope (SEM) image of the fabric with CNTs coated on the surface depicts the formation of the conductive network. The surface and even the grooves between the conjunction fabric fibers are coated with CNTs (Figure 1d), which guarantee both good conductivity and excellent mechanical stability of the electrode.

The working mechanism of the WET can be concluded as a single-electrode mode by referring to the four working modes of the TENG.<sup>24</sup> Human skin and silk textile are regarded as the two friction layers in this situation. Figure 1e presents the charge distribution (top) and simulation of the electrostatic potential distribution (bottom) during the electricity generation progress of the WET. Briefly, the skin and the silk will obtain an equal amount of positive and negative charges after several frictional cycles with each other due to their different tribo-polarities (Figure 1e,(i)).<sup>25</sup> Once the skin approaches the silk, electrons will flow from the ground to the CNT electrode to balance the potential difference between the two layers (Figure 1e,(ii)). There is no current in the circuit when skin is in full

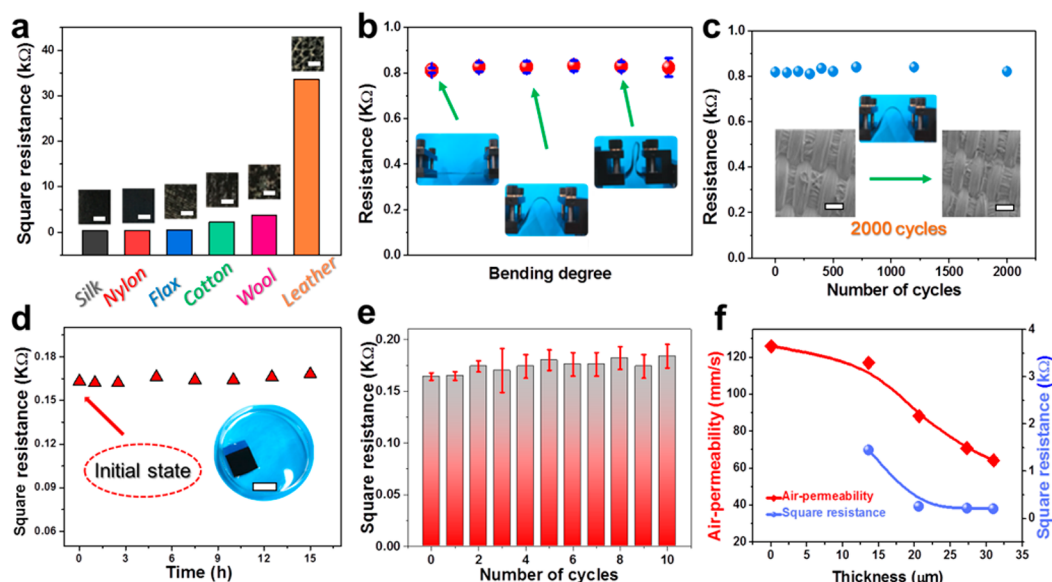


**Figure 2.** Electric properties and air permeability of the CNT electrode. (a) Sheet resistances and optical photographs (insets) of the CNT electrode on different fabric substrates (scale bars, 5 mm). (b) Resistances of the electrode on nylon substrate when variable degrees of bending. (c) Stability of the electrode on a nylon substrate. The insets are SEM images of the electrode on the nylon substrate before and after 2000 bending cycles (scale bars, 200  $\mu\text{m}$ ). (d) Resistances of the electrode after being immersed in water for different times. The inset is the photograph of the electrode immersed in water for 1 week (scale bars, 20 mm). (e) Resistances of the same electrode on the nylon substrate after being immersed in water for different times and 2 h for each time. (f) Air permeability of the nylon textile and conductivity of the electrode with different CNT ink thicknesses.

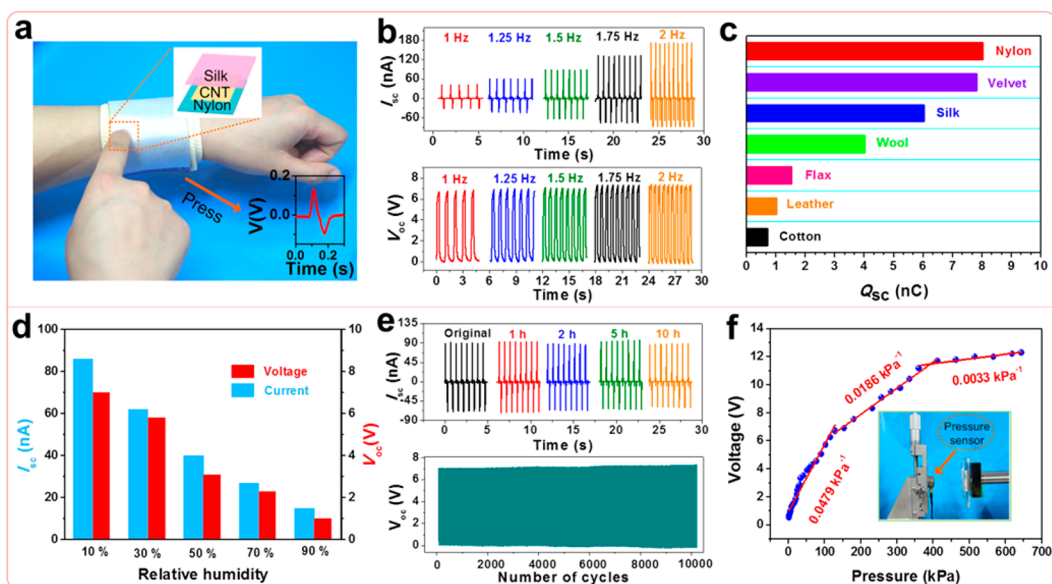


**Figure 3.** Characterizing the electrical performance of the WET. (a) Schematic diagram of the process to produce a signal of the WET. (b)  $I_{sc}$  and  $V_{oc}$  of the WET with different frequencies. (c)  $Q_{sc}$  of the WET fabricated by different textiles when rubbed with copper film. (d)  $I_{sc}$  and  $V_{oc}$  of the WET under various relative humidities. (e) Top:  $I_{sc}$  of the WET after being dipped in water for different times and dried in air. Bottom: Stability of the WET. (f) Pressure sensitivity of the WET. The inset is the optical photograph of the experimental setup.

contact with the silk because the bound charges on the surfaces of the two are almost in neutralization (Figure 1e,(iii)). Moreover, electrons will gradually flow back to the ground when skin departs from the silk (Figure 1e,(iv)). This is a full cycle of the signal generation process for the vertical single-electrode mode WET, and the working mechanism of the in-plane single-electrode mode WET in one sliding cycle is depicted in Figure S2 (Supporting Information).

The performance of the screen-printed electrode is systematically discussed in this work. First, the square resistances of

CNT ink printed on various kinds of fabrics were investigated to seek a suitable substrate. As presented in Figure 2a, except for leather, the square resistances of the electrodes based on different textiles have negligible differences. The high square resistance of the leather-based electrode can be attributed to the furrow distributed in the fabric (inset in Figure 2a), which leads to the disconnection of the CNT ink. Due to the flexible textile substrate like nylon, the electrode shows outstanding mechanical performance. The resistance between the two corners (diagonal line) of the electrode ( $5 \times 8 \text{ cm}^2$ ) almost



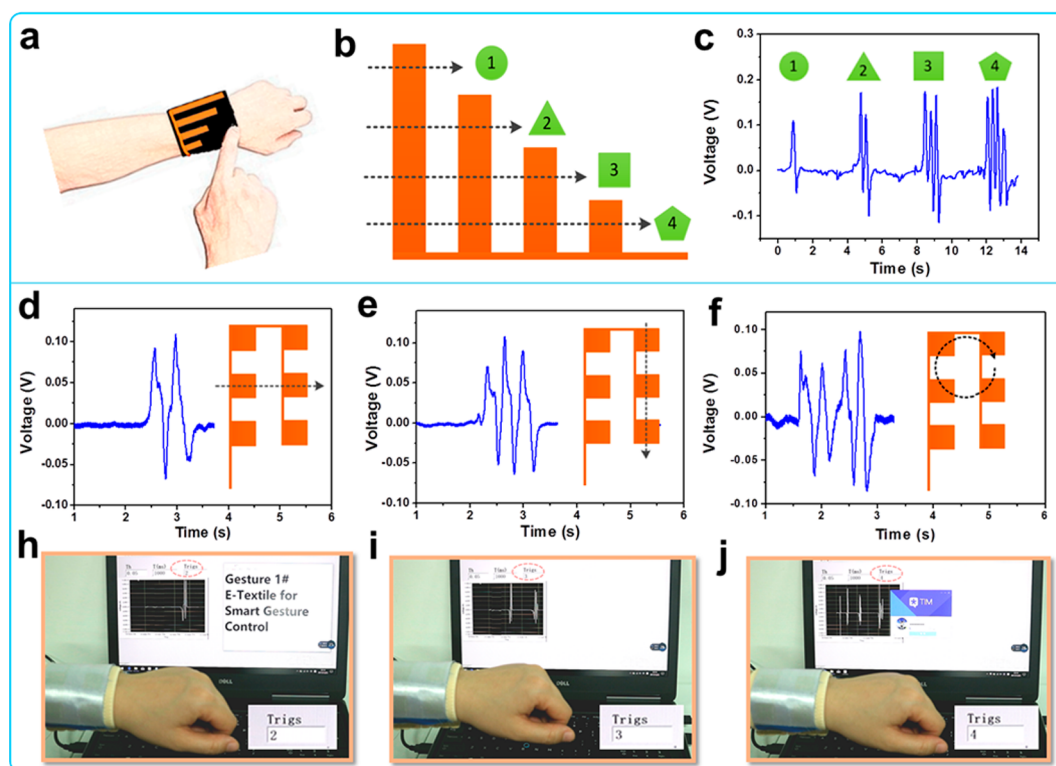


**Figure 4.** Diversity of the WET and demonstrations of the WET in accessing software. (a) Diagrammatic drawing of a striped array WET incorporated into a wristband. The paths of fingertip sliding (b) and corresponding signals (c) of the WET. (d–f) Paths of finger sliding and corresponding signals of a squared array WET. (h,i) Demonstration of the squared array WET controlling software.

remains stable upon different bending angles, even when the electrode is folded (Figure 2b). The phenomenon can be attributed to the PU added in the CNT ink, which is an elastomer and can prevent the whole electrode from cracking. The stability of the electrode was measured, as well. After repeated bending for over 2000 cycles, the resistance between the two corners of the electrode ( $5 \times 8 \text{ cm}^2$ ) shows few signs of decline. The insets in Figure 2c are the SEM images of the surface of the electrode in the initial state (left) and that after 2000 bending cycles (right). The comparison of the two images indicates no obvious difference, which is further evidence for the excellent durability of the electrode.

In order to demonstrate the washable property of the electrode, the square resistances of the electrode were tested after being immersed in water for different times. The square resistance shows no trend of decline (Figure 2d). The inset is the optical photograph of the electrode after being immersed in water for 1 week, from which we can see that the water is limpid and no CNTs seem to detach from the nylon substrate. Moreover, the square resistance of the same electrode dipped in the water several times (2 h for each time) was explored. As presented in Figure 2e, the square resistance of the electrode shows negligible variation, revealing that the electrode can be soaked for a long time and repeatedly.

It is predicted that the thickness of the CNT layer will influence both the conductivity of the electrode and the air permeability of the textile. Therefore, both conductivity and air permeability of the electrode are evaluated and presented in Figure 2f. The thickness of the CNTs can be controlled by printing for different times. As the thickness of the CNT layer increases, the square resistance of the electrode decreases at first and then reaches saturation. This phenomenon can be

explained by the fact that the conductive network of the electrode has been established at the thickness of  $20 \mu\text{m}$ . Conversely, the air permeability of the textile presents a declining trend with the thickness of the CNTs coated on the textile increasing. However, the air permeability of the textile with the CNT thickness of around  $20 \mu\text{m}$  ( $88.6 \text{ mm/s}$ ) is comparable to that of the primitive textile, which is able to meet the requirement of being breathable for human skin. For reference, air permeability of jeans is  $26.4 \text{ mm/s}$ . Considering the conductivity and breathability of the electrode, a  $20 \mu\text{m}$  thick CNT layer is adopted in the following experiments.

Based on the electrode demonstrated above and contact electrification, the WET is capable of generating electrical signals when pressed with a finger (Figure 3a). To measure the output performance of the WET, a copper film ( $2 \times 2 \text{ cm}^2$ ) and a linear motor were utilized to simulate the skin and drive the device, respectively. First, the output performances of the WET with different frequencies are measured to investigate the frequency response of the sensor (Figure 3b). The results show that the open-circuit voltage ( $V_{oc}$ ) of the device remains stable under various frequencies, whereas the short-circuit current ( $I_{sc}$ ) of the WET shows a linear relationship with the frequency increasing from 1 to 2 Hz. The signals under varied frequencies demonstrate both fast response and stability of the WET, which ensure the practicality of the WET for working as a sensor for further applications.

Even though everything in the world has frictional property, the transferred friction charges are various among different materials due to their varied ability to capture electrons.<sup>25</sup> Here, a series of textiles were used to fabricate WETs, which cooperate with the copper film to construct the contact-separation mode. The results provided in Figure 3c

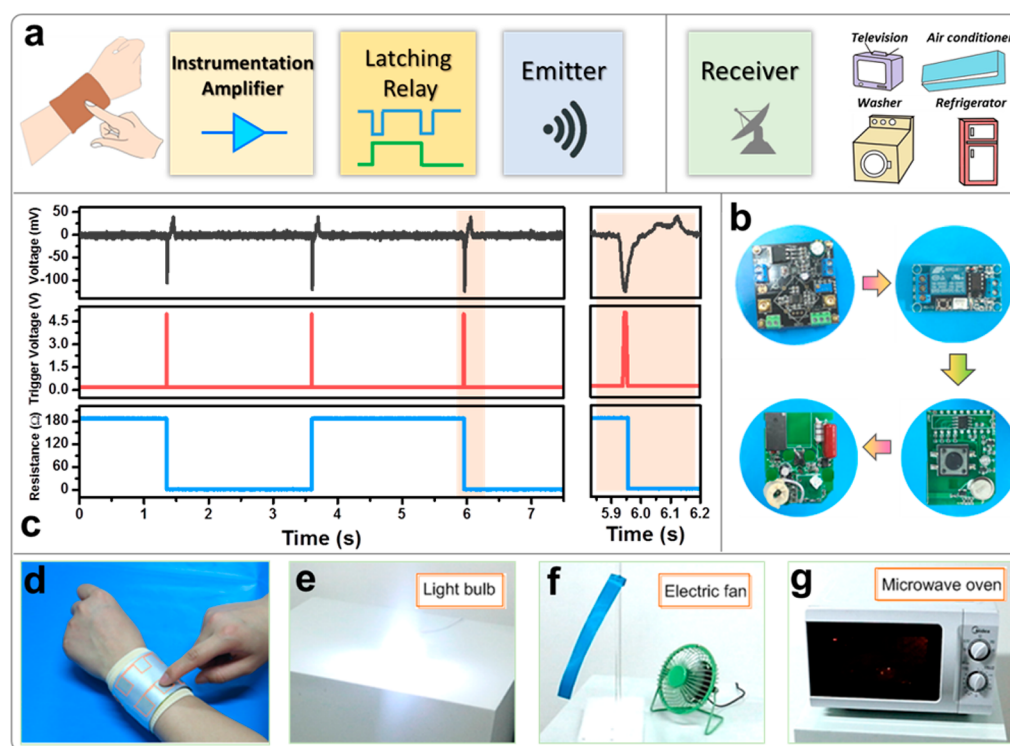


**Figure 5.** Application of the WET in a wireless smart home control system. (a) Scheme diagram of a WET involved in a smart home control system. Utilizing several simple electric modules, a pressing signal can be converted into a trigger signal to control the appliances. (b) Optical photographs of the electron components used in the circuit of the home control system. (c) From top to bottom, the original signals of pressing, amplified/converted trigger signals, and the state of parallel resistance connected with the relay. (d–g) Demonstration of the WET in controlling a light bulb, an electric fan, and a microwave oven.

demonstrated that the textile with fiber content of nylon is more tribo-positive, whereas that of cotton is more tribo-negative among the seven fabrics. However, all of the textiles are able to generate friction charges, which indicate the universality and diversity of the fabric for the WET. Here, we just adopt silk as one typical example to fabricate the WET. It should be noted that the outputs of the WET fabricated by different textiles have no obvious relationship with the thickness. For example, the output of the WET fabricated with wool (average thickness, 6.0 mm) is 3 times higher than that fabricated with cotton (average thickness, 3.8 mm).

As the humidity around us changes, the electric performance of the WET was investigated by varying the relative humidity in a test environment. Figure 3d shows that the  $I_{sc}$  and  $V_{oc}$  of the WET at a relative humidity of 90% have dropped significantly compared with those at a relative humidity of 10%. The increased humidity of the environment diminishes the outputs of the WET, which should be caused by the screening effect of water molecules.<sup>26</sup> Notably, the output signal still can be distinguished at a relatively high humidity (90%), indicating that this device can work in high humidity. In order to demonstrate the washability and stability of the WET, the  $I_{sc}$  of the WET was recorded after being immersed in water for different times and then dried in air (Figure 3e, top). The  $I_{sc}$  of the WET remains almost unchanged even the steeping time increased from 2 to 15 h, which firmly proves the washability of the E-textile. Moreover, the durability of the WET was tested for more than 10 000 cycles with contact-separation motion. The  $V_{oc}$  of the WET provided in Figure 3e (bottom) shows no tendency to degrade, which provides further evidence for the durability and reliability of the WET. The pressure sensitivity of

the device is discussed, as well (Figure 3f). According to the results of linear fitting, the sensitivity of the WET can be divided into three parts, including 0.0479, 0.0186, and 0.0033  $\text{kPa}^{-1}$ , which is in accord with previous work.<sup>27</sup> The high sensitivity of the WET can be attributed to the rough surface constituted of numerous microfibers of textile and CNTs.

Due to the feasibility of screen-printing, the WET is able to be fabricated with an arbitrary array for gesture sensing. Here, the WETs with a striped array and squared array are listed as two typical examples to demonstrate their application in controlling software on the computer. As displayed in Figure 4a, the WET with a striped array and a fingertip constitute the signal source. The motion paths of the fingertip and corresponding signals are provided in Figure 4b,c, respectively. Owing to the varied lengths of the strips, the motion trajectory of the fingertip starting at different position leads to a voltage waveform with different signal numbers. The detailed electricity generation process of the WET based on in-plane sliding mode is shown in Figure S2 (Supporting Information). It should be noticed that the voltage signal of the striped array WET was the record of the voltage drop across a resistor (20  $\text{M}\Omega$ ). Similarly, the fingertip motion paths on a squared array WET (2  $\times$  3 pixels) and corresponding real-time signals were measured. Figure 4d–f and Figure S3 show the voltage waveform with 2–6 signal responses to various fingertip movements. After connecting the WET with a computer, a human–machine interface is established on the basis of the software platform Labview. As a consequence, various finger gestures are able to control different software. For example, two signals generated by a fingertip sliding from the left to the right of the squared array WET are able to open a TXT file (Figure 4h). The TXT

file will be closed after three signals were obtained through finger sliding from top to bottom of the squared array WET (Figure 4i). Similarly, chatting software was accessed with four signals generated by a cycle path of the fingertip (Figure 4j). The relative video is provided in Movie S1 in the Supporting Information. A WET with a flower-like electrode array is put forward to further demonstrate the diversity of the WET, and different numbers of signals can be realized through different sliding angles of the fingertip. The corresponding real-time signals can be found in Figure S4 (Supporting Information).

Our WET can also act as a touch tribo-sensor to establish a wireless smart home controlling system. As depicted in Figure 5a, the WET incorporated into a wristband can perceive the touch by human fingertips, thus generating a pulse signal, which is able to wirelessly trigger home appliances with the utilization of some electronic modules. Optical photographs of the small circuit boards used in this work are presented in Figure 5b, which include an AD623, a relay, an emitter, and a receiver. On the basis of these circuits, the original pulse signals were converted into trigger signals. As is depicted in Figure 5c, from top to bottom, the first signal is the original signal of pressing, followed by amplified/converted trigger signals and state of parallel resistance connected with the relay. The emitter and receiver is serially connected with the relay and home appliance, respectively. Once the WET generates a pulse signal, the state of relay is supposed to switch. As a consequence, the receiver will obtain the signal sent by the emitter and further control the electric appliance. Demonstrations of the WET in controlling a light bulb, electric fan, and microwave oven are shown Figure 5d–g. The related videos can be found in Movies S2, S3, and S4 in the Supporting Information. Moreover, the application of the WET is not limited to smart home control, which can also be extended to factories, hospitals, railway stations, and so forth.

## CONCLUSION

In summary, a washable electronic textile has been demonstrated to serve as a self-powered gesture/touch sensor for intelligent human–machine interactions. The washable, breathable, and designable electrode is fabricated through screen-print CNT ink, which not only has excellent flexibility and stability but also guarantees relatively high conductivity (0.2 k $\Omega$ /sq) and air permeability (88.2 mm/s). Attributed to the rough surface constituted of numerous microfibers of the textile and CNTs, the WET shows high sensitivity and fast response to external mechanical force. Based on the single-electrode mode, the fabricated WET with an electrode array can work as a self-powered gesture sensor to access software on the computer. Moreover, the WET incorporated into clothes can serve as a smart home control system, which can easily wirelessly control appliances such as a light bulb, electric fan, microwave oven, and so forth. Considering the advantages of being durable through washing, low cost, available for mass production, and skin-friendly, the WET shows great potential in multifunctional wearable devices and human–machine interface systems.

## METHODS

**Synthesis of the CNT Ink.** Two grams of CNTs and 0.5 g of dispersant for CNTs were dissolved in 12.5 g of deionized water in a beaker. After being stirred at room temperature for 30 min, 15 g of PU emulsion with solid content of 40% was added to the beaker and stirred for another 30 min. Subsequently, the mixed solution was

further treated through an ultrasonic dispersing machine, and the conductive CNT ink was obtained.

**Fabrication of the TENG.** The width of the striped array electrode was 1.5 cm with a height of 2, 4, 6, and 8 cm. The space between the two strips is 1.5 cm, as well. The squared electrode array was fabricated with 2  $\times$  3 pixels, and the side length of each square is 1.5 cm. In addition, the space between the two squares is 1.5 cm. The electrodes were printed on the surface of the textile substrate. After being heated at the temperature of 80  $^{\circ}$ C for 10 min, the CNTs were anchored on the surface of the textile. The upper textile was placed above the electrodes, and then the three layers were integrated into one layer through a hot-press machine (120  $^{\circ}$ C, 1 min). All textiles adopted in this work were brought randomly. The average thickness of silk, nylon, flax, cotton, wool, leather, and velvet is about 1.2, 2.1, 4.0, 6.0, 5.3, and 3.8 mm, respectively.

**Signal Processing Circuit.** The raw signal of the WET generated through pressing was amplified and converted to a trigger by being connected with an AD623-based instrumentation-amplifying circuit. After that, the signal was converted to a trigger and that connected with a relay in series. The relay is further connected with an emitter in series. The receiver is serially connected to a home appliance.

**Characterization and Electrical Measurements.** The SEM image of the surface of the textile with CNTs was taken with a Hitachi SU8020. The open-circuit voltage and short-circuit current of the device were measured with a Keithley electrometer system (Keithley 6514). The square resistance of the electrode was measured by a four-point probe (RTS-9). The air permeability of the textile was measured by a TEXTTEST AG (FX 3300) at a test area and pressure of 5 cm<sup>2</sup> and 100 Pa, respectively. The thickness of the CNT layer was measured by a thickness tester (CHY-CA).

## ASSOCIATED CONTENT

### Supporting Information

The Supporting Information is available free of charge on the ACS Publications website at DOI: 10.1021/acsnano.8b02477.

Figures S1–S4 and notes providing the formation of a mechanism of the washability of the WET; the electricity generation process of the WET based on in-plane sliding mode; paths of the figures and corresponding signals of the 2  $\times$  3 pixel array WET; schematic diagram and real-time signals of the flower-like array WET (PDF)

Movie S1: Demonstration of finger gestures to control different software (AVI)

Movie S2: Demonstration of the WET controlling a light bulb (AVI)

Movie S3: Demonstration of the WET controlling an electric fan (AVI)

Movie S4: Demonstration of the WET controlling a microwave oven (AVI)

## AUTHOR INFORMATION

### Corresponding Authors

\*E-mail: jnwangjn@sina.com.

\*E-mail: cqphysicsghy@126.com.

\*E-mail: congjuli@126.com

### ORCID

Xinyu Du: 0000-0003-1101-7409

Zuqing Yuan: 0000-0003-3988-0618

Chi Zhang: 0000-0002-7511-805X

Congju Li: 0000-0001-6030-7002

Zhong Lin Wang: 0000-0002-5530-0380

### Notes

The authors declare no competing financial interest.



## ACKNOWLEDGMENTS

The authors are thankful for support from the Beijing Natural Science Foundation (No. 2182014), the National Natural Science Foundation of China (NSFC Nos. 51503005, 21703010, and 21274006), National Key R&D Project from Minister of Science and Technology (2016YFA0202702, 2016YFA0202703, and 2016YFA0202704), the Programs for Beijing Science and Technology Leading Talent (Grant No. Z161100004916168), the Beijing Hundred, Thousand and Ten Thousand Talent Project (110403000402), the General Program of Science and Technology Development Project of Beijing Municipal Education Commission of China (SQKM201710012004), Beijing Institute of Fashion Technology special fund translation for the construction of high-level teachers (BIFTQG201801), and the “Thousands Talents” Program for Pioneer Researcher and His Innovation Team, China.

## REFERENCES

- (1) Zeng, W.; Shu, L.; Li, Q.; Chen, S.; Wang, F.; Tao, X. M. Fiber-Based Wearable Electronics: A Review of Materials, Fabrication, Devices, and Applications. *Adv. Mater.* **2014**, *26*, 5310–5336.
- (2) Carey, T.; Cacovich, S.; Divitini, G.; Ren, J.; Mansouri, A.; Kim, J. M.; Wang, C.; Ducati, C.; Sordan, R.; Torrisi, F. Fully Inkjet-Printed Two-Dimensional Material Field-Effect Heterojunctions for Wearable and Textile Electronics. *Nat. Commun.* **2017**, *8*, 1202.
- (3) Fan, H.; Li, K.; Li, Q.; Hou, C.; Zhang, Q.; Li, Y.; Jin, W.; Wang, H. Prepolymerization-Assisted Fabrication of an Ultrathin Immobilized Layer to Realize a Semi-Embedded Wrinkled AgNW Network for a Smart Electrothermal Chromatic Display and Actuator. *J. Mater. Chem. C* **2017**, *5*, 9778–9785.
- (4) Lipomi, D. J.; Vosguerichian, M.; Tee, B. C. K.; Hellstrom, S. L.; Lee, J. A.; Fox, C. H.; Bao, Z. Skin-Like Pressure and Strain Sensors Based on Transparent Elastic Films of Carbon Nanotubes. *Nat. Nanotechnol.* **2011**, *6*, 788–792.
- (5) Kim, C. C.; Lee, H. H.; Oh, K. H.; Sun, J. Y. Highly Stretchable, Transparent Ionic Touch Panel. *Science* **2016**, *353*, 682–687.
- (6) Hu, L.; Choi, J. W.; Yang, Y.; Jeong, S.; La Mantia, F.; Cui, L. F.; Cui, Y. Highly Conductive Paper for Energy-Storage Devices. *Proc. Natl. Acad. Sci. U. S. A.* **2009**, *106*, 21490–21494.
- (7) Hu, S.; Rajamani, R.; Yu, X. Flexible Solid-State Paper Based Carbon Nanotube Supercapacitor. *Appl. Phys. Lett.* **2012**, *100*, 104103.
- (8) Pu, X.; Li, L.; Song, H.; Du, C.; Zhao, Z.; Jiang, C.; Cao, G.; Hu, W.; Wang, Z. L. A Self-Charging Power Unit by Integration of a Textile Triboelectric Nanogenerator and a Flexible Lithium-Ion Battery for Wearable Electronics. *Adv. Mater.* **2015**, *27*, 2472–2478.
- (9) Liu, M.; Pu, X.; Jiang, C.; Liu, T.; Huang, X.; Chen, L.; Du, C.; Sun, J.; Hu, W.; Wang, Z. L. Large-Area All-Textile Pressure Sensors for Monitoring Human Motion and Physiological Signals. *Adv. Mater.* **2017**, *29*, 1703700.
- (10) Dadgostar, F.; Sarrafzadeh, A. Gesture-Based Human–Machine Interfaces: A Novel Approach for Robust Hand and Face Tracking. *Iran J. Comput. Sci.* **2018**, *1*, 47.
- (11) Alcoverro, M.; Suau, X.; Morros, J. R.; López-Méndez, A.; Gil, A.; Ruiz-Hidalgo, J.; Casas, J. R. Gesture Control Interface for Immersive Panoramic Displays. *Multimed. Tools Appl.* **2014**, *73*, 491–517.
- (12) Lin, Z.; Yang, J.; Li, X.; Wu, Y.; Wei, W.; Liu, J.; Chen, J.; Yang, J. Large-Scale and Washable Smart Textiles Based on Triboelectric Nanogenerator Arrays for Self-Powered Sleeping Monitoring. *Adv. Funct. Mater.* **2018**, *28*, 1704112.
- (13) Fan, F.-R.; Tian, Z.-Q.; Lin Wang, Z. Flexible Triboelectric Generator. *Nano Energy* **2012**, *1*, 328–334.
- (14) Wang, Z. L. Catch Wave Power in Floating Nets. *Nature* **2017**, *542*, 159–160.
- (15) Lee, J. H.; Hinchet, R.; Kim, T. Y.; Ryu, H.; Seung, W.; Yoon, H. J.; Kim, S. W. Control of Skin Potential by Triboelectrification with Ferroelectric Polymers. *Adv. Mater.* **2015**, *27*, 5553–5558.
- (16) Chen, H.; Xu, Y.; Bai, L.; Jiang, Y.; Zhang, J.; Zhao, C.; Li, T.; Yu, H.; Song, G.; Zhang, N.; Gan, Q. Crumpled Graphene Triboelectric Nanogenerators: Smaller Devices with Higher Output Performance. *Adv. Mater. Technol.* **2017**, *2*, 1700044.
- (17) Khan, U.; Kim, T. H.; Ryu, H.; Seung, W.; Kim, S. W. Graphene Tribotronics for Electronic Skin and Touch Screen Applications. *Adv. Mater.* **2017**, *29*, 1603544.
- (18) Seung, W.; Gupta, M. K.; Lee, K. Y.; Shin, K. S.; Lee, J. H.; Kim, T. Y.; Kim, S.; Lin, J.; Kim, J. H.; Kim, S. W. Nanopatterned Textile-Based Wearable Triboelectric Nanogenerator. *ACS Nano* **2015**, *9*, 3501–3509.
- (19) Dong, K.; Deng, J.; Zi, Y.; Wang, Y. C.; Xu, C.; Zou, H.; Ding, W.; Dai, Y.; Gu, B.; Sun, B.; Wang, Z. L. 3D Orthogonal Woven Triboelectric Nanogenerator for Effective Biomechanical Energy Harvesting and as Self-Powered Active Motion Sensors. *Adv. Mater.* **2017**, *29*, 1702648.
- (20) Chen, J.; Huang, Y.; Zhang, N.; Zou, H.; Liu, R.; Tao, C.; Fan, X.; Wang, Z. L. Micro-Cable Structured Textile for Simultaneously Harvesting Solar and Mechanical Energy. *Nat. Energy* **2016**, *1*, 16138.
- (21) Wen, Z.; Yeh, M.-H.; Guo, H.; Wang, J.; Zi, Y.; Xu, W.; Deng, J.; Zhu, L.; Wang, X.; Hu, C.; Zhu, L.; Sun, X.; Wang, Z. L. Self-Powered Textile for Wearable Electronics by Hybridizing Fiber-Shaped Nanogenerators, Solar Cells, and Supercapacitors. *Sci. Adv.* **2016**, *2*, e1600097.
- (22) Chen, M.; Li, X.; Lin, L.; Du, W.; Han, X.; Zhu, J.; Pan, C.; Wang, Z. L. Triboelectric Nanogenerators as a Self-Powered Motion Tracking System. *Adv. Funct. Mater.* **2014**, *24*, 5059–5066.
- (23) Pu, X.; Guo, H.; Chen, J.; Wang, X.; Xi, Y.; Hu, C.; Wang, Z. L. Eye Motion Triggered Self-Powered Mechnosensational Communication System Using Triboelectric Nanogenerator. *Sci. Adv.* **2017**, *3*, e1700694.
- (24) Zhang, C.; Tang, W.; Han, C.; Fan, F.; Wang, Z. L. Theoretical Comparison, Equivalent Transformation, and Conjunction Operations of Electromagnetic Induction Generator and Triboelectric Nanogenerator for Harvesting Mechanical Energy. *Adv. Mater.* **2014**, *26*, 3580–3591.
- (25) Wang, Z. L. Triboelectric Nanogenerators as New Energy Technology for Self-Powered Systems and as Active Mechanical and Chemical Sensors. *ACS Nano* **2013**, *7*, 9533–9557.
- (26) Pu, X.; Liu, M.; Chen, X.; Sun, J.; Du, C.; Zhang, Y.; Zhai, J.; Hu, W.; Wang, Z. L. Ultrastretchable, Transparent Triboelectric Nanogenerator as Electronic Skin for Biomechanical Energy Harvesting and Tactile Sensing. *Sci. Adv.* **2017**, *3*, e1700015.
- (27) Yang, Z. W.; Pang, Y.; Zhang, L.; Lu, C.; Chen, J.; Zhou, T.; Zhang, C.; Wang, Z. L. Tribotronic Transistor Array as an Active Tactile Sensing System. *ACS Nano* **2016**, *10*, 10912–10920.